Fatigue Analysis of Printed PLA using Neural Networks

Moises Jimenez-Martinez, *Member, IAENG,* Sergio G. Torres-Cedillo, and Jacinto Cortés-Pérez

***Abstract*—The implementation of additive manufacturing as a disruptive process for the development of components has generated the need to know manufacturing parameters to obtain mechanical properties similar to or better than those of conventional processes. Thus, the improvement and optimisation of materials used have aroused interest in converting Polylactic acid (PLA) 3d printed parts from prototyping to functional components. In this regard, they must withstand cyclical loads. To do so, conventional methods must consider all variables used in the manufacturing process. Herein, we propose the use of neural networks to perform mechanical fatigue analysis of the printed components of PLA. The mechanical behaviour of the printed components was expressed for the neural network as parameters based on quasistatic tests, and the output of the network was the expected fatigue life in cycles. The initial quasistatic behaviour of the 3d printed parts was linearly elastic. However, a viscoelastic behaviour developed over time. The discharge time between charging cycles influenced the cumulative damage process. According to the experimental results and their correlations, the fatigue life of printed components can be predicted using neural networks by achieving an average error of 1.59% .**

***Index Terms*—Additive Manufacturing; Neural Network; Mechanical Fatigue; cumulative damage; PLA**

I. Introduction

THE latest evolution in manufacturing has introduced an additive manufacturing (AM) process, which involves joining materials and building components from three-dimensional data. The components are split into a code, resulting in the slicing of the model into different layers as functions of printed parameters. Then, shapes are done layer by layer in a plane (x- and y-directions). The movement of the bed connects the layers in the z-direction, creating a three-dimensional (3d) component.

Because of the flexibility of AM with Polylactic acid (PLA), it can be used in low production to customise components [1], in automotives to generate lightweight structures to reduce CO_2 emissions [2], in building spare components and rapid prototyping [3], [4] and in aeronautical applications. It can also be used in biomedicine for surgical instruments, such as implants to reduce the time of manufacturing [5]. AM with PLA has great application opportunities in the above fields due to its high level of adaptation, as in ankle-foot orthosis [6] and porous scaffolds in hard tissue because of its biocompatibility [7], in addition to industrial customised components.

However, these components of polymeric materials have to overcome certain mechanical behaviours, such as low elastic moduli, which affect applications where the components have spatial constraints due to tolerance or assembly functions. Another effect of AM is that it generates a thermal history through the fusion process of the filament as its heating, melting and cooling processes modify microstructures, which also change as a function of build orientation [8]. Although the flexibility of AM enables it to generate organic and optimised models without the need to modify and manufacture tools, it has detrimental effects on the control of mechanical properties, such as endurance strength to cyclic loads, as in the case of long-term applications. In contrast to static loads, there is much less information about the effects of fatigue response on 3d printed components, which are essential for predicting their dynamic behaviour as functional components [9].

In implementing Fused filament fabrication (FFF) printed components of PLA in industrial applications, numerical tools and design procedures are necessary to predict mechanical responses and durability. Otherwise, these components would remain applied in nonstructural components [10]. Like metals, plastics develop accumulated damage for cyclic loads, where nucleating microcracks grow until fatigue failure is reached [11].

As illustrated in Figure 1, the structural analyses for durability assessments needs to consider designs, materials. The environment can modify loads and influences materials [12]. In this regard, the manufacturing process depends on the parameters of AM printing. The parameters related to construction affect its mechanical properties. These factors comprise layer width, the direction of each layer (raster), layer height, and filament angle—each of which can have an impact on quasistatic properties [13]. Meanwhile, the tensile strength and Young's modulus of fused deposition modelling $AM - PLA$ materials increase as a function of the load direction [14], [15].

Structural analyses for durability assessments must consider designs, materials, loads and manufacturing processes (Fig. 1). The environment can modify such loads but also influences the materials [12]. In this regard, the manufacturing process depends on the AM printing parameters. The parameters related to a construction affect its mechanical properties. These include the layer width, direction of each layer (raster), layer height and filament angle, which affect quasistatic properties [13]. Meanwhile, the tensile strength and Young's modulus of fused deposition modelling $AM - PLA$ materials increase as a function of the load direction [14]. Moreover, compressive mechanical behaviour

Manuscript received October 9, 2023; revised April 30, 2024.

This work was supported in part by the Kautex lightweight structures lab at Tecnologico de Monterrey, with the sponsorship of Kautex Textron GmbH.

M. Jimenez-Martinez is a Professor of School of Engineering and Science, Tecnologico de Monterrey, Puebla, Mexico (corresponding author; e-mail: moisesjimenezmartinez@gmail.com).

Sergio G. Torres-Cedillo is Professor at FES Aragon - UNAM, Edo. Mex. 57171 México (e-mail: sergiotorres98@aragon.unam.mx).

Jacinto Cortés-Pérez is head of the technnology Center at FES Aragon - UNAM, Edo. Mex. 57171 México (e-mail: jacop@unam.mx).

is linearly dependent on the density [16]. The combination of these layer parameters influences material bonding. Depending on the infill density and the printing pattern, air can be left trapped, similar to voids in casting. The linear pattern results in the highest tensile modulus, possibly because of the smaller spaces between individual layers than other patterns [15]. This affects the component with a different structure along the section and in the boundary, causing an anisotropic behaviour [17].

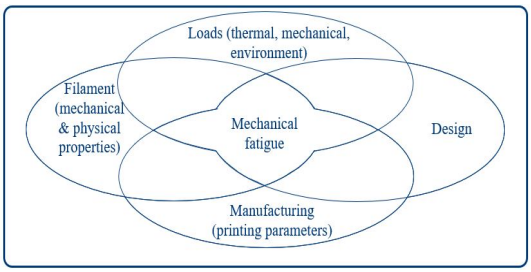

Fig. 1: Mechanical fatigue assessment in 3d printed components

A combination of experimental–computational and analytical methods may be utilised to facilitate a systematic approach using the V-model (Fig. 2). The development of a component starts from dimensional constraints and functional requirements. The material to be used is defined depending on the operational characteristics and functional requirements. At this point, we begin to develop the manufacturing strategy, which defines the printing parameters, leading us to a printed component. Properties such as surface finish and mechanical properties are evaluated, and quasistatic, transient or dynamic tests are performed to evaluate the performance of the final component. If any changes are required, the printing parameters are changed.

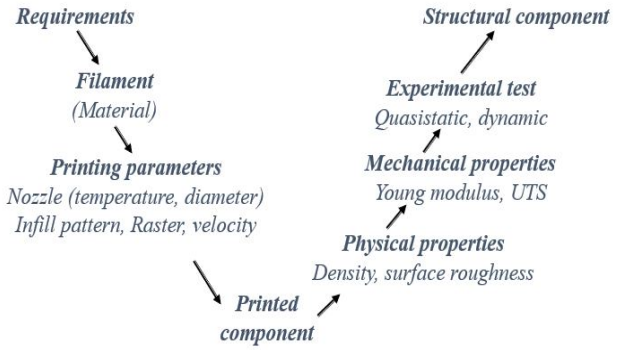

Fig. 2: Analysis process for AM printed components using V-model

Fig. 3 shows the schematic printing process and its main components. The FFF process transports the filament through the feeding system, where it is heated to melt, and extruded through the nozzle to generate the component on the platform.

Although the initial stress–strain behaviour of thermoplastic such as PLA is linearly elastic, a nonlinear development of viscoelasticity happens gradually with time [18]. Thermoplastic materials used in FFF have a strong dependence on polymers based on the strain rate and frequency load [19].

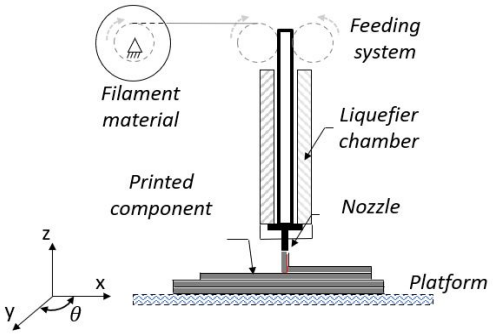

Fig. 3: Schematic printing process

The best configurations of the printing components for cyclic loads are 45°/− 45° longitudinal fibres and transversals, respectively (Fig. 4). These were based on the stress tensor [20]. From a fatigue design perspective, $AM - PLA$ can be treated as a homogeneous and isotropic material [21]. Although a solid component is desired to prevent internal crack nucleation, the manufacturing process itself generates a different behaviour depending on the printing direction and parameters.

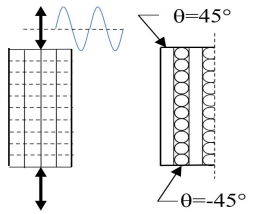

Fig. 4: Schematic layers in printed component for a raster angle of 45°

Therefore, the introduction of an artificial neural network (ANN) to predict the fatigue life of PLA printed components is proposed. In this respect, fatigue tests have been performed using the staircase method. Based on the complex process of printing a component with the printing parameters, in addition to the nonlinear behaviour of the thermoplastic, the quasistatic mechanical response of the printed component must be considered to predict the fatigue strength using a neural network.

II. Fatigue assessment using an ANN

Conventionally manufactured polymeric materials have superior fatigue performance than printed materials. The influences of the printing process and filament used significantly impact their durability [22], [23]. However, despite considerable advancements in AM techniques, 3d-printed parts still face issues related the fatigue life according to the thermal process generated during their processing. This depends not directly on the microstructure as in a typical alloy with different phases but on the formed internal geometry due to the filament. Although cumulative damage models can be used to predict fatigue life, the number of variables in the 3d printed components creates a need for improvements in fatigue life prediction processes. Thus, machine learning models such as artificial intelligence have been used to reduce the time and development cost in AM to improve

not only its geometry but also the printing parameters and the component quality [24], [25], [26].

The present study employs a multilayer neural network to establish a non-parametric model for predicting fatigue life. This network is conceptualized as a fully connected network, wherein each neuron in every layer is linked to every other neuron in the adjacent forward layer, as illustrated in Fig. 5. The training of the network employs a backpropagation algorithm, requiring a set of training data composed of input/target vector pairs. A target vector is defined as the desired output post-training, while the output vector is generated using the current neural network. The backpropagation process consists of three stages: (i) forward transmission involves computing the output signal at each network layer, (ii) calculating and providing feedback on the error between the output and target vectors, and (iii) adjusting the weights. In stage (i), the computation entails outputting weighted signals from the initial network layer to the final layer. Stage (ii) is where network training utilizes optimization techniques to minimize the associated error by adjusting network weights and biases. This adjustment is iterated for subsequent training pairs [27], [28].

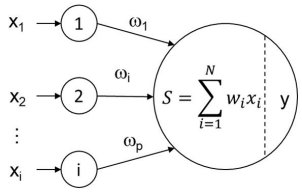

Fig. 5: Schematic neuron

With reference to Fig. 6, let $S^{(j)}$ be the number of neurons in the j^{th} layer, and let J be the total number of layers. If $y_n^{(j)}$ is the $S^{(j)} \times 1$ vector comprising the signal outputs of the j^{th} layer, then:

$$a_k^{(j)} = y_n^{(j)} \tag{1}$$

$$a_k^{(1)} = g^{(1)}\left(W^{(1)}x_k + b^{(1)}\right) \tag{2}$$

$$a_k^{(j)} = g^{(j)}\left(W^{(j)}a_k^{j-1} + b^{(j)}\right), j = 2, ...J \tag{3}$$

In this context, the inputs x_k encompass load amplitude, mechanical properties (Young's modulus and ultimate tensile strength), strain (elastic and plastic), and absorbed energy. The relationships between these inputs and the desired output y_k correspond to the cycles resulting from the experimental tests. The terms $W^{(j)}$ and $b^{(j)}$ represent the matrix of weights and vector of biases, respectively, for j_{th} layer. Additionally, $g^{(j)}$ is a vector operator comprising the transfer functions of the neurons of the j^{th} layer.

For a given user-prescribed architecture, the Artificial neural network (ANN) underwent training with input/output data. The training procedure employed the Bayesian regularization backpropagation [28] to determine optimal weights and biases. This optimization aimed to minimize the mean square error δ between the output of the network y_n^j and the actual data (i.e. target) output for a given input x_k. With reference to Fig. 6, the current feedforward network consists

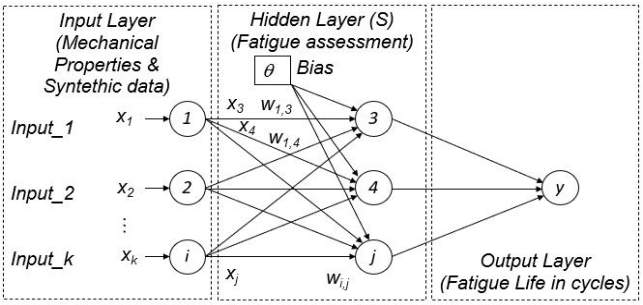

Fig. 6: Multilayer neural network

of only one hidden layer with 44 neurons, utilizing a binary sigmoid transfer function to activate the neurons.

III. Additive manufacturing

All specimens in this study were printed using an Ender printer with a red colour plus filament. The print setup utilized a raster angle of 45° with a solid infill density set at 100%. The material properties of the PLA utilized include a diameter of $1.75mm$, a printing temperature of 200^oC, a bed temperature of 55^oC, and a density of $1.24g/cm^3$.

IV. Experimental tests

Three specimens were tested at $1.25mm/min$ to understand the mechanical behaviour of the printed PLA components. The mechanical behaviours of the engineering and true curves are shown in Fig. 7. Table I summarises the results of the ultimate tensile strength, fracture stress, strain at fracture, initial Young's modulus and that after a softening in the mechanical response. One advantage of the true strain–stress curve is that it improves the analysis of the tensile test by considering the change in the transverse area during the test.

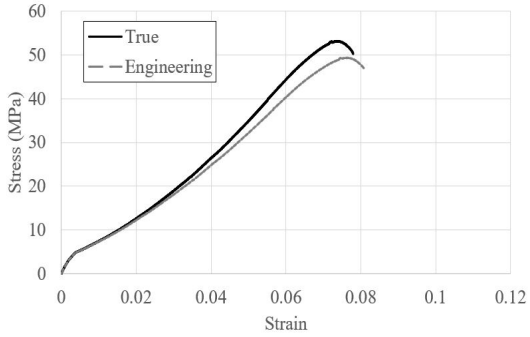

Fig. 7: Results of the tensile test

TABLE I: Summary results of the tensile tests.

Specimen	UTS_{True}	σ_{fTrue}	ε_{fTrue}	E_o	E_M
1	53.14	46.43	0.081	2751.428	1756.8
2	48.23	43.11	0.076	1866	1654.8
3	48.19	47.14	0.078	2093.33	1642.8
Ave	48.85	45.56	0.0759	2236.9	1133.2

The process of accumulated damage depends on the loads applied and the properties of the material, not only on its strength but also on how it is recovered during discharge. The recoverability depends on the elastic behaviour of the

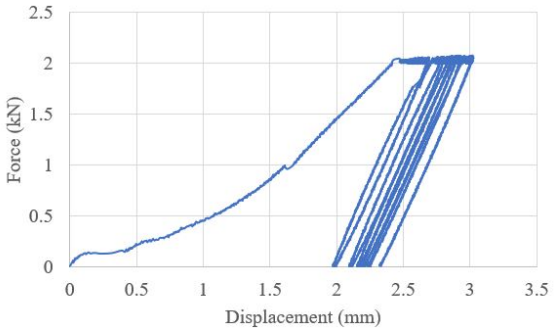

(a) force vs. displacement

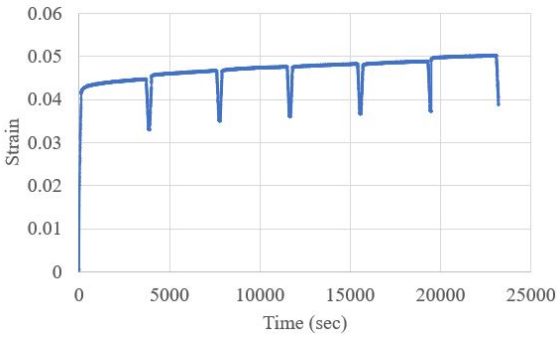

(b) strain as a time function

Fig. 8: Creep at 2000 N

material and on how the layers interact in dissipating energy. Thus, load control tests were performed at 2000 N (Fig. 8) and 3000 N (Figures 9–11) to understand the cyclic behaviour and the dissipated energy. First, a ramp on load control was applied and defined until it reached the expected load. Then, the load was kept constant to measure the strain response. This was repeated until the component was broken.

Tests were conducted at various discharge times to understand the recovery processes of PLA. This allowed them to assess whether a longer unloading time contributed to the total deformation tolerated by the components. Fig. 9 has an unloading time of 10 min between loads, Fig. 10 has an unloading time of 30 min and Fig. 11 has an unloading time of 60 min. The limitation of this approach is that in a cyclic time history, there is no constant unloading time. The most striking result that emerged from the Figures at $3000N$ was that the permanent deformation occurred at a strain of $0.033 \pm 0/0.002$.

The strain reached was major when there was a greater unloading time. This also increased that tolerated by the quasistatic cycle based on the recovery. Using equation 4, the dissipated energy was obtained and used as input in the neural network.

$$U_o = \frac{\sigma_x^2}{2E} \tag{4}$$

Fig. 12a shows the creep test at 3500 N until failure. Meanwhile, Fig. 12b can be related to the strain behaviour of the material fatigue response. The tests revealed a small period of crack nucleation, followed mostly by propagation and a sudden failure. This behaviour was opposite to those of metallic materials, where most of the life component was required for crack initiation.

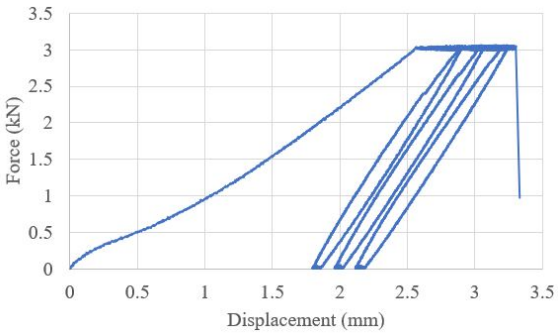

(a) force vs. displacement

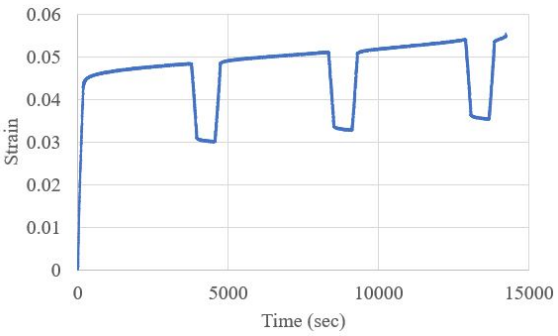

(b) strain as a function of time

Fig. 9: Creep at 3000N unload 10 minutes

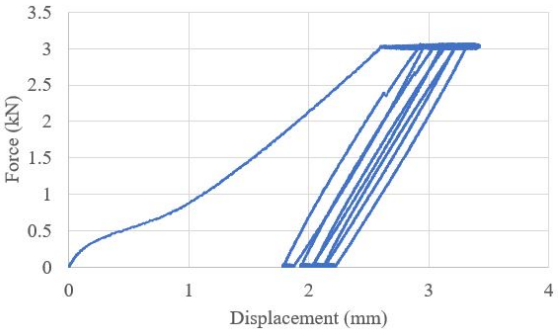

(a) force vs. displacement

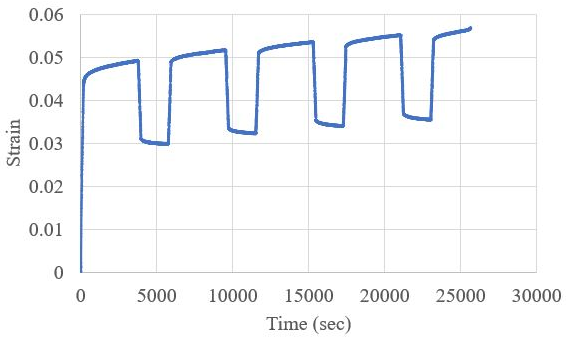

(b) strain as a function of time

Fig. 10: Creep at 3000N unload 30 minutes

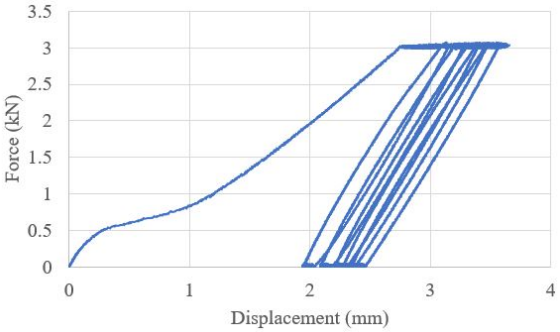

(a) force vs. displacement

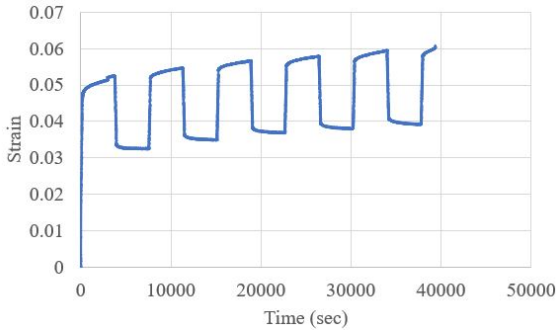

(b) strain as a function of time

Fig. 11: Creep at 3000N unload 60 minutes

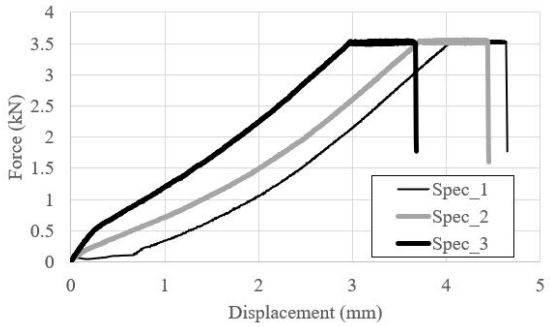

(a) force vs. displacement

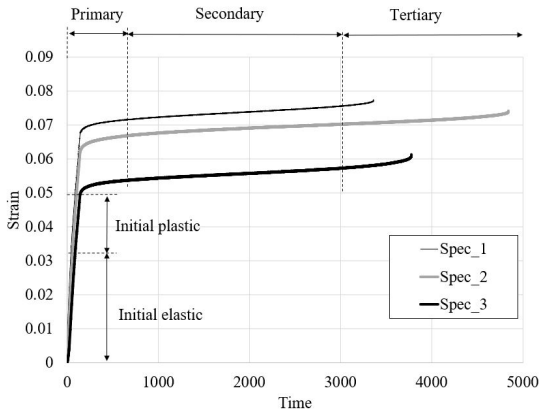

(b) strain as a function of time

Fig. 12: Creep at 3.5kN until failure

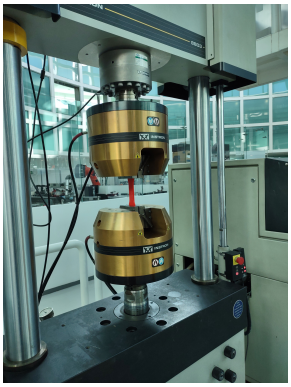

(a) uniaxial test machine

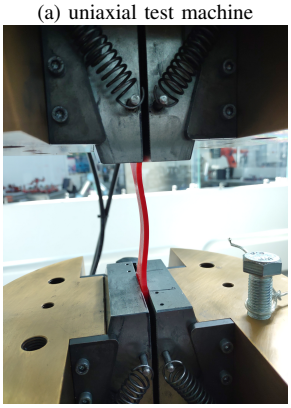

(b) specimen under test

Fig. 13: Fatigue tests

Training the neural network with more material information is proposed to use parameters based on the strain. The first is the relationship between the elastic strain (ε_{elas}) and plastic strain ε_{plas} of the mean values in Fig. 12b.

$$\varepsilon_c = \frac{\varepsilon_{elas}}{\varepsilon_{plas}} \tag{5}$$

Another parameter proposed is the ratio of the permanent strain of the creep test at the first unloading (ε_p) and the strain at the fracture (ε_f) from table I using the following equation:

$$\varepsilon_c = \frac{\varepsilon_p}{\varepsilon_f} \tag{6}$$

Fig. 13 shows the experimental setup for the fatigue tests, which were performed using a uniaxial Instron test machine. Fig. 13b shows the component at compression load. Based on the expected behaviour expressed in Fig. 12 and the mechanism of failure propagation, the test was run until an increment of $\pm 0.5mm$ mm of displacement.

V. Results and Discussion

The fatigue test results are summarised in Fig. 14 using an S–N curve. The mean values per load level were evaluated using an ANN and linear damage rule (LDR), the parameters for the $S-N$ curve for this assessment is defined in the range of high cycle fatigue [20], the expected cycles are described by Miner's rule, as is expressed by:

$$N_2 = N_1 \left(\frac{S_1}{S_2}\right)^k \tag{7}$$

where n_i is the number of repetitions during the operation and N_i are the repetitions tolerated and the amplitude S at ith load level.

The results of the correlational analysis are compared in table II, where a significant positive correlation between the experimental results and the prediction using ANN was found.

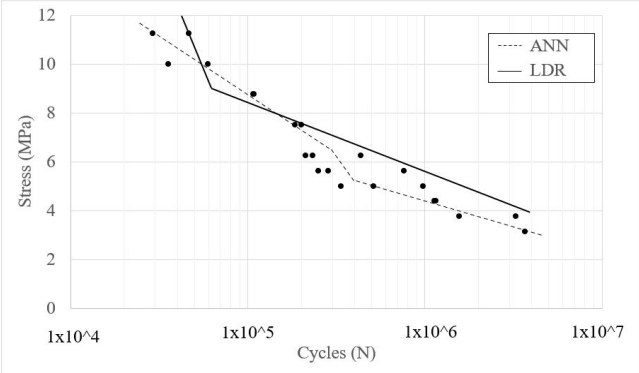

Fig. 14: S-N curve for printed PLA components

In order to analyze the cyclic behaviour, the failure area has been evaluated as is shown in Fig. 15. Ductile failure is presented by a slow progression of the failure propagation (Fig.15a). While the fragile failure is rapidly spreading, generating a shiny surface. The process of failure by cyclic load can be observed by patterns where it is observed how the failure zone increases after the load is again applied (Fig.15b), until it reaches a critical parameter (Fig.16).

TABLE II: Fatigue life prediction using Linear Damage rule and Artificial Neural Network

Load	Cycles	LDR	ANN
500	3,683,006	6,157,265	3,683,006
600	2,422,194	2,062,056	2,422,194
700	1,140,484	1,020,736	1,140,484
800	609,455	637,092	583,696
900	431,701	420,372	381,072
1000	293,305	289,807	293,305
1200	193,442	152,265	193,442
1400	107,673	88,364	107,673
1600	47,469	72,953	47,469
1800	37,840	65,801	37,840

In summary, these results showed a softening in the PLA printed component. This affected the component stiffness. Although the UTS found reached a value of 48.8 MPa and the Young's modulus was 1.36 GPa, the UTS was 10.9% more than that reported by [29]. The difference was that the true strain–stress curve was used for the fatigue damage evaluation, and the scatter present in this additive process for the parameters is described in Fig. 1.

In the case of the Young's modulus, the initial value of 2.23 GPa was not used; instead, we used the value of 1.13 GPa after a softening. This was around 5% more than that reported by [29]. This process of softening agreed with the change in behaviour to a nonlinear response in viscoelastic thermoplastics after time load [18]. It is important to use the value of Young's modulus after softening because it expresses the change in stiffness of the material found in both static and cyclic tests. Thus, using quasistatic tests can develop relationships that can be used to predict fatigue life using $(ANNs)$.

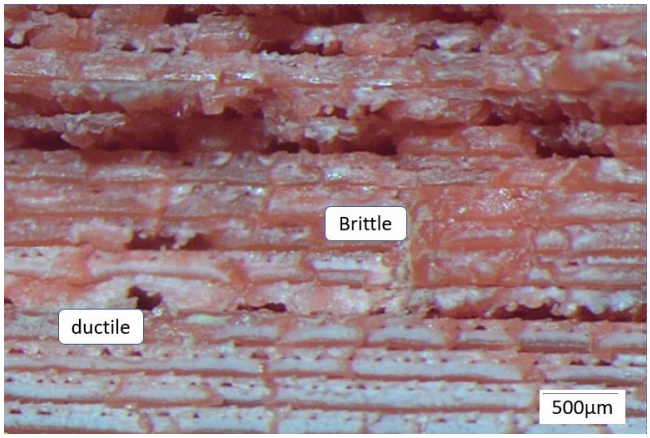

(a) brittle and ductile behaviour

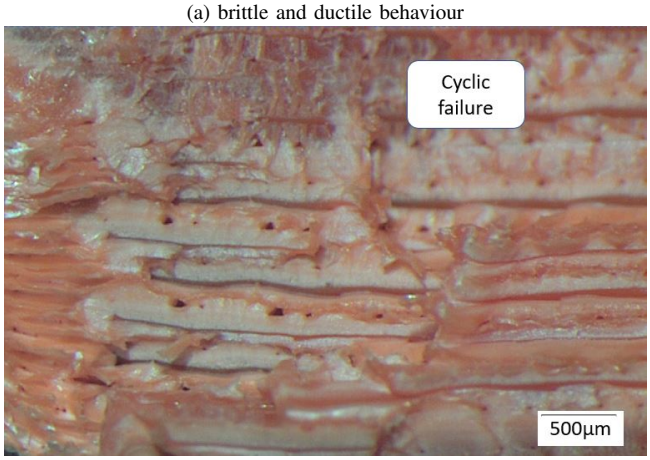

(b) cyclic failure

Fig. 15: Failure analysis

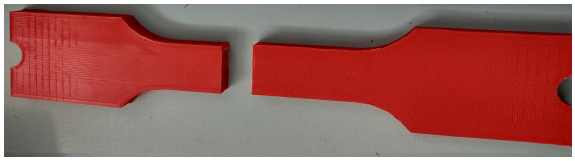

Fig. 16: Failure in component

VI. Conclusions

In this work, the accumulated damage process was analysed in printed parts of PLA. Mechanical properties obtained for the quasistatic tests were used to understand the printed PLA. Fatigue life prediction in thermoplastics like PLA is complex as they initially behave linearly, but this behaviour changes over time to a nonlinear response due to their viscoelastic response. Meanwhile, ANNs can be used to perform fatigue assessments. The prediction using $(ANNs)$ has an error of 1.59%, using an accumulated damage rule the error is 26.7%. Thus, extrapolating the network prediction is not possible because of the nonlinear behaviour of thermoplastics for quasistatic and dynamic loads, which depends on all variables related to the time, time at load level, strain rate, unloaded time and frequency load. Notwithstanding the relatively limited sample, this work offers valuable insights into the analysis of the fatigue life of PLA printed components.

REFERENCES

[1] T. D. Ngo, A. Kashani, G. Imbalzano, K. T. Nguyen, and D. Hui, "Additive manufacturing (3d printing): A review of materials, methods, applications and challenges," *Composites Part B: Engineering*, vol. 143, pp. 172–196, 2018.

[2] H. Hegab, N. Khanna, N. Monib, and A. Salem, "Design for sustainable additive manufacturing: A review," *Sustainable Materials and Technologies*, vol. 35, p. e00576, 2023.

[3] K. Kanishka and B. Acherjee, "A systematic review of additive manufacturing-based remanufacturing techniques for component repair and restoration," *Journal of Manufacturing Processes*, vol. 89, pp. 220–283, 2023.

[4] J. Krishnaraj and K. Harshavardhan Reddy, "Modelling and additive manufacturing of a four stroke petrol engine using pla material," *Materials Today: Proceedings*, 2023.

[5] A. Yadollahi and N. Shamsaei, "Additive manufacturing of fatigue resistant materials: Challenges and opportunities," *International Journal of Fatigue*, vol. 98, pp. 14–31, 2017.

[6] M. Azadi and A. Dadashi, "Fatigue and impact properties of 3d printed pla reinforced with kenaf particles," *Journal of Materials Research and Technology*, vol. 16, pp. 461–470, 2022.

[7] R. Bakhshi, M. Mohammadi-Zerankeshi, M. Mehrabi-Dehdezi, R. Alizadeh, S. Labbaf, and P. Abachi, "Additive manufacturing of pla-mg composite scaffolds for hard tissue engineering applications," *Journal of the Mechanical Behavior of Biomedical Materials*, vol. 138, p. 105655, 2023.

[8] K. Markandan and C. Q. Lai, "Fabrication, properties and applications of polymer composites additively manufactured with filler alignment control: A review," *Composites Part B: Engineering*, vol. 256, p. 110661, 2023.

[9] S. Ford and T. Minshall, "Invited review article: Where and how 3d printing is used in teaching and education," *Additive Manufacturing*, vol. 25, pp. 131–150, 2019.

[10] O. Lampron, A. Lingua, D. Therriault, and M. Lévesque, "Characterization of the non-isotropic tensile and fracture behavior of unidirectional polylactic acid parts manufactured by material extrusion," *Additive Manufacturing*, vol. 61, p. 103369, 2023.

[11] L. Safai, J. S. Cuellar, G. Smit, and A. A. Zadpoor, "A review of the fatigue behavior of 3d printed polymers," *Additive Manufacturing*, vol. 28, pp. 87–97, 2019.

[12] O. Menezes, T. Roberts, G. Motta, M.-H. Patrenos, W. McCurdy, A. Alotaibi, M. Vanderpool, M. Vaseghi, A. Beheshti, and K. Davami, "Performance of additively manufactured polylactic acid (pla) in prolonged marine environments," *Polymer Degradation and Stability*, vol. 199, p. 109903, 2022.

[13] R. Teharia, R. M. Singari, and H. Kumar, "Optimization of process variables for additive manufactured pla based tensile specimen using taguchi design and artificial neural network (ann) technique," *Materials Today: Proceedings*, vol. 56, pp. 3426–3432, 2022, first International Conference on Design and Materials.

[14] Y. Zhao, Y. Chen, and Y. Zhou, "Novel mechanical models of tensile strength and elastic property of fdm am pla materials: Experimental and theoretical analyses," *Materials Design*, vol. 181, p. 108089, 2019.

[15] C. Abeykoon, P. Sri-Amphorn, and A. Fernando, "Optimization of fused deposition modeling parameters for improved pla and abs 3d printed structures," *International Journal of Lightweight Materials and Manufacture*, vol. 3, no. 3, pp. 284–297, 2020.

[16] R. Cláudio, J. Dupont, R. Baptista, M. Leite, and L. Reis, "Behaviour evaluation of 3d printed polylactic acid under compression," *Journal of Materials Research and Technology*, vol. 21, pp. 4052–4066, 2022.

[17] J. Plocher and A. Panesar, "Review on design and structural optimisation in additive manufacturing: Towards next-generation lightweight structures," *Materials Design*, vol. 183, p. 108164, 2019.

[18] A. H. Foroughi, C. Valeri, D. Jiang, F. Ning, M. Razavi, and M. J. Razavi, "Understanding compressive viscoelastic properties of additively manufactured pla for bone-mimetic scaffold design," *Medical Engineering Physics*, vol. 114, p. 103972, 2023.

[19] M. Česnik, J. Slavič, and M. Boltežar, "Accelerated vibration-fatigue characterization for 3d-printed structures: Application to fused-filament-fabricated pla samples," *International Journal of Fatigue*, vol. 171, p. 107574, 2023.

[20] M. Jimenez-Martinez, J. Varela-Soriano, J. J. R. Carreón, and S. G. Torres-Cedillo, "Mechanical fatigue of pla in additive manufacturing," *Engineering Failure Analysis*, vol. 149, p. 107273, 2023.

[21] O. Ezeh and L. Susmel, "Fatigue strength of additively manufactured polylactide (pla): effect of raster angle and non-zero mean stresses," *International Journal of Fatigue*, vol. 126, pp. 319–326, 2019.

[22] V. Shanmugam, O. Das, K. Babu, U. Marimuthu, A. Veerasimman, D. J. Johnson, R. E. Neisiany, M. S. Hedenqvist, S. Ramakrishna, and F. Berto, "Fatigue behaviour of fdm-3d printed polymers, polymeric composites and architected cellular materials," *International Journal of Fatigue*, vol. 143, p. 106007, 2021.

[23] M. Azadi and A. Dadashi, "Experimental fatigue dataset for additive-manufactured 3d-printed polylactic acid biomaterials under fully-reversed rotating-bending bending loadings," *Data in Brief*, vol. 41, p. 107846, 2022.

[24] M. Parsazadeh, S. Sharma, and N. Dahotre, "Towards the next generation of machine learning models in additive manufacturing: A review of process dependent material evolution," *Progress in Materials Science*, vol. 135, p. 101102, 2023.

[25] Z. Zhan and H. Li, "A novel approach based on the elastoplastic fatigue damage and machine learning models for life prediction of aerospace alloy parts fabricated by additive manufacturing," *International Journal of Fatigue*, vol. 145, p. 106089, 2021.

[26] M. Jimenez-Martinez and M. Alfaro-Ponce, "Fatigue damage effect approach by artificial neural network," *International Journal of Fatigue*, vol. 124, pp. 42–47, 2019.

[27] N. M. O'Dowd, R. Madarshahian, M. S. H. Leung, J. Corcoran, and M. D. Todd, "A probabilistic estimation approach for the failure forecast method using bayesian inference," *International Journal of Fatigue*, vol. 142, p. 105943, 2021.

[28] C. C. Aggarwal, *Neural Networks and Deep Learning*, 2nd ed. Springer Nature Switzerland AG, 2023.

[29] S. Rodríguez-Reyna, C. Mata, J. Díaz-Aguilera, H. Acevedo-Parra, and F. Tapia, "Mechanical properties optimization for pla, abs and nylon + cf manufactured by 3d fdm printing," *Materials Today Communications*, vol. 33, p. 104774, 2022.